DELFT UNIVERSITY OF TECHNOLOGY

REPORT 11-01

A SCALABLE HELMHOLTZ SOLVER COMBINING THE SHIFTED LAPLACE PRECONDITIONER WITH MULTIGRID DEFLATION

A.H. Sheikh D. Lahaye C. Vuik

ISSN 1389-6520

Reports of the Department of Applied Mathematical Analysis

Delft 2011

A Scalable Helmholtz Solver Combining the Shifted Laplace Preconditioner With Multigrid Deflation

A.H. Sheikh, D. Lahaye, C. Vuik

April 11, 2011

Abstract

A Helmholtz solver whose convergence is parameter independent can be obtained by combining the shifted Laplace preconditioner with multigrid deflation. To proof this claim, we develop a Fourier analysis of a two-level variant of the algorithm proposed in [1]. In this algorithm those eigenvalues that prevent the shifted Laplace preconditioner from being scalable are removed by deflation using multigrid vectors. Our analysis shows that the spectrum of the two-grid operator consists of a cluster surrounded by a few outliers, yielding a number of outer Krylov subspace iterations that remains constant as the wave number increases. Our analysis furthermore shows that the imaginary part of the shift in the two-grid operator can be made arbitrarily large without affecting the convergence. This opens promising perspectives on obtaining a very good preconditioner at very low cost. Numerical tests for problems with constant and non-constant wave number illustrate our convergence theory.

1 Introduction

The aim of this work is to develop a highly performant iterative solution algorithm for the finite difference discretized Helmholtz equation modeling wave propagation on large scale. The efficient solution of this problem has long been an open problem. It indeed appears that an increase in the wave number in almost all of the currently available solvers leads to a large increase in the number of iterations and therefore in computational cost. With the appearance of shifted Laplace preconditioners however, a computationally feasible solution has become available.

The first papers on these preconditioners are [2] and [3] in which a Laplace operator and a Laplace operator with a real shift, respectively, are proposed. Both preconditioners lead to good results for medium size wave numbers. For large wave numbers numerical results on the contrary show a steep increase in the number of iterations. With the Laplace preconditioners with a complex shift proposed and studied in [4–6], the solver requires a number of iterations that grows only linearly as the wave number increases. Inspired by this work, a number of generalizations appeared shortly afterwards in [1, 7–10] together with applications in different industrial contexts in [11–18]. The convergence of the shifted Laplace preconditioners is analyzed in [19–21]. This analysis shows that the smallest eigenvalues of the preconditioned operator rush to zero as the wave number increases and explains the non-scalability. In [1,22], the authors therefore propose to combine the shifted Laplace preconditioner with a multigrid deflation operator. The latter can be seen as a second level preconditioner that removes small eigenvalues. The resulting method is quite involved and requires a flexible Krylov subspace method. Numerical results however show that the required number of iterations is almost independent of the wave number. An overview of preconditioners for the Helmholtz equation finally is given in [23].

In this paper we analyze a simplified two-level variant of the method proposed in [1], in which both the shifted Laplace preconditioner and coarse grid system required by the second level preconditioner are inverted by a direct method. We associate to the shifted Laplace preconditioner the role of a smoother and perform a Fourier two-grid analysis of one-dimensional model problem with Dirichlet boundary conditions. This Fourier analysis results in a closed form expression for the eigenvalues of the two-grid operator and shows that the number of iterations of Krylov subspace methods does not increase with the wave number. The analysis also shows that the shifted Laplace preconditioner can be made arbitrarily diagonally dominant by increasing the imaginary part of the shift without paying any penalty in the number of Krylov subspace iterations. We subsequently apply our solver to two-dimensional model problems with constant and non-constant wave number discretized by a second order finite difference scheme on uniform meshes. Numerical results confirm the theoretical analysis.

The paper is structured as follows. In Section 2 we describe a Helmholtz problem with and without heterogeneity, its computational domain and its second order finite difference discretization. In Section 3 the shifted Laplace preconditioner and multigrid deflation are introduced. Theoretical results of the Fourier analysis of a one-dimensional Helmholtz problem are presented in Section 4. In Section 5 numerical results supporting the theory are shown and finally conclusions are drawn in Section 6.

2 Problem Formulation

The Helmholtz equation for the unknown field $u(x, y)$ on a two-dimensional domain Ω with boundary $\partial\Omega$ reads

$$-\Delta u - k^2 u = g\,, \tag{1}$$

where $k(x, y)$ and $g(x, y)$ are the wave number and the source function, respectively. The wave number k, the frequency f and angular frequency $\omega = 2\pi f$, the speed of propagation $c(x, y)$ and the wavelength $\lambda = \frac{c(x,y)}{f}$ are related by

$$k = \frac{2\pi}{\lambda} = \frac{\omega}{c}\,. \tag{2}$$

On the boundary $\partial\Omega$ we impose either homogeneous Dirichlet or first order Sommerfeld radiation boundary conditions. Denoting the imaginary unit by ι, the latter are given by

$$\frac{\partial u}{\partial n} - \iota k u = 0\,. \tag{3}$$

We will consider two model problems. In the first we set $\Omega = (0, 1) \times (0, 1)$, the wave number constant and source equal to the Dirac delta function

$$g(x, y) = \delta(x - \frac{1}{2}, y - \frac{1}{2})\,. \tag{4}$$

For convergence analysis we will consider a one-dimensional variant of this problem.

As second problem we consider the so-called wedge-problem introduced in [24] in which $\Omega = (0, 600) \times (0, 1000)$ is subdivided into three layers as shown in Figure 1(a). In each layer the wave velocity c is constant with the value shown in the same figure. A point source is centered in $x = 300$ and $y = 0$. The real part of the computed solution is shown in Figure 1(b).

The finite difference discretization of the model problems on a mesh with mesh width h in both x and y direction has the following stencil

$$[A_h] = \frac{1}{h^2}\begin{bmatrix} 0 & -1 & 0 \\ -1 & 4-\kappa^2 & -1 \\ 0 & -1 & 0 \end{bmatrix}, \tag{5}$$

where $\kappa = k\,h$, and leads to a system of linear equations

$$A_h x_h = b_h, \tag{6}$$

where the discrete Helmholtz operator A_h is the sum of a stiffness matrix $-\Delta_h$ and $-k^2$ times the identity I_h

$$A_h = -\Delta_h - k^2 I_h\,. \tag{7}$$

For the discretization scheme, h is chosen by the rule of thumb of using at least 10 nodes per wave length, which leads to the restriction

$$\kappa \approx \frac{2\pi}{10} \approx 0.628\,. \tag{8}$$

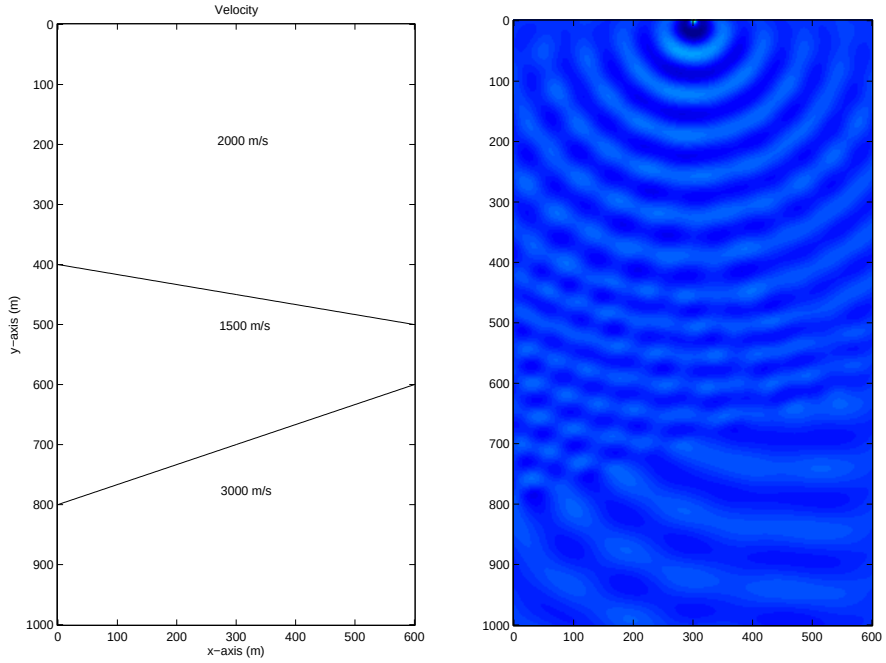

(a) Domain of the wedge problem with velocity c in each layer.

(b) Real part of the computed solution.

Figure 1: The wedge problem introduced in [24].

3 Two-grid Deflated Shifted Laplace Preconditioner

The linear system matrix A_h in (6) is complex-valued, sparse, symmetric, non-Hermitian and indefinite. The number of negative eigenvalues increases with the wave number k. Solving this linear system on large scale necessarily requires the use of iterative solution techniques. GMRES [25] and Bi-CGSTAB [26] are suitable choices for this system. Krylov subspace methods, in general, converge well for systems with a favorable spectrum. Such a spectrum can be obtained using preconditioning and deflation. In this work we make use of the shifted Laplace preconditioner (SLP) combined with multigrid deflation.

3.1 Shifted Laplace Preconditioner

The shifted Laplace preconditioners are among the most effective preconditioners for the Helmholtz equation. Their development started with the preconditioner obtained by discretizing Laplace operator ($M_h = -\Delta_h$) as proposed in [2]. Later the Helmholtz operator with opposite sign in front of the wave number ($M_h = -\Delta_h + k^2 I_h$) was considered in [3]. Subsequently a Laplace operator with a complex shift was introduced in [4, 27] and found to be more effective. Denoting by β_1 and β_2 two real numbers, the complex shifted Laplace preconditioner can be written as

$$M_{h,(\beta_1,\beta_2)} = -\Delta_h - (\beta_1 - \iota\beta_2)k^2 I_h, \qquad \beta_1, \beta_2 \in \mathbb{R}. \tag{9}$$

The complex shift introduces damping and renders the preconditioned system amenable to approximate inversion using either geometric multigrid [1,27] or MILU [28]. More recently algebraic multigrid has been used to invert the preconditioner [8,9]. In this paper we limit ourselves to the exact inversion of $M_{h,(\beta_1,\beta_2)}$.

The spectral properties of the shifted Laplace preconditioned Helmholtz operator $M^{-1}_{h,(\beta_1,\beta_2)}A_h$ are elaborated in [19] where it is shown that the spectrum consists of a cluster near one, and some eigenvalues that lie at the distance of $O(\epsilon/k^2)$ from the origin where ϵ is a small number depending upon k. The eigenvalues are bounded above by one but the smallest eigenvalues rush to zero as k increases. This is illustrated in Figure 2. With an increase in k, the very small eigenvalues cause the convergence of the outer Krylov subspace iteration to slow down. This justifies to consider the matrix $M_{h,(\beta_1,\beta_2)}$ given by (9) to define a splitting of A^h and to refer to the stationary iterative method with error propagation matrix $S_{h,(\beta_1,\beta_2)}$ given by

$$S_{h,(\beta_1,\beta_2)} = I_h - M^{-1}_{h,(\beta_1,\beta_2)}A_h\,, \tag{10}$$

as a *smoother*. In this paper the increase in number of Krylov subspace iterations caused by small eigenvalues is handled by multigrid deflation.

3.2 Two-grid Deflation

Deflation is a technique to deal with small eigenvalues (in the preconditioned system) that adversely affect the convergence of a Krylov subspace iteration [29,30]. The basic idea is to bring the small eigenvalues to zero by a projection procedure. Denoting the size of A_h by n, we define the matrix $Z_h \in \mathbb{R}^{n\times r}$ whose $r < n$ columns are the deflation vectors. These vectors should be chosen such that the Galerkin or coarse level matrix $E_h = Z_h^T\, A_h\, Z_h$ is non-singular. In the particular case that A_h is real, symmetric and positive definite, this requirement is met if Z_h has full column rank. Given Z_h, we define the deflation operator $P_h \in \mathbb{C}^{n\times n}$ as

$$P_h = I_h - Q_h\, A_h \text{ where } Q_h = Z_h\, E_h^{-1}\, Z_h^T \text{ and } E_h = Z_h^T\, A_h\, Z_h\,. \tag{11}$$

Observe that Q^h inherits the complex symmetry from A^h. It is an easy to verify that P_h is a projection and that its spectrum consists of 0 and 1.

In this paper we will perform multigrid deflation by coarsening the grid by a factor of two in each coordinate direction and setting the matrix Z_h in (11) equal to the coarse to fine grid bilinear interpolation operator I_H^h. With this choice the deflation operator P_h defined by (11) coincides with the two-grid correction operator, i.e.,

$$P_{h,H} = I_h - Q_h\, A_h \text{ where } Q_h = I_H^h A_H^{-1} I_h^H \text{ and } A_H = I_h^H A_h I_H^h\,. \tag{12}$$

For large problems, the exact inversion of A_H^{-1} is impractical and one has to resort to approximate solvers instead. Without proper care, this will however lead to the introduction of close to zero eigenvalues in the preconditioned systems. This can be avoided by controlling the approximate solve with A_H or by deflating to the largest eigenvalue of the preconditioned system. In this paper we limit ourselves to the exact inversion of A_H.

3.3 Two-grid Preconditioner

The operator resulting from applying a two-grid deflation step after a a shifted-Laplace pre-smoothing step will be denoted as

$$B_{h,H,(\beta_1,\beta_2)} = P_{h,H} S_{h,(\beta_1,\beta_2)} \,. \tag{13}$$

In the remainder of this paper we will show by Fourier analysis and by numerical experiments that using this operator as a preconditioner for GMRES, will result in a scalable solver in the sense that the number of iterations remains constant as the wave number increases.

4 Fourier Two-Grid Analysis

For an analysis of the two-grid preconditioner $B_{h,H,(\beta_1,\beta_2)}$ defined by (13), we consider the Helmholtz equation on the domain $\Omega = (0,1)$ supplied with homogeneous Dirichlet boundary conditions. These boundary conditions are easier to analyze. Furthermore, as Dirichlet boundary conditions do not introduce any wave damping, the analysis that follows can be considered to be a worst-case analysis for the problem with Sommerfeld boundary conditions. This is illustrated by Table 1 and Table 2.

Assuming p to be a non-zero natural number, we discretize Ω by uniform mesh with $n = 2^p$ elements and with mesh width $h = 1/n$. Standard $h \rightarrow H = 2h$ coarsening of the fine mesh denoted by Ω^h will result in a coarse mesh denoted by Ω^H. Second order finite difference discretization on Ω^h with stencil

$$[A_h] = \frac{1}{h^2} \left[\begin{array}{ccc} -1 & 2-\kappa^2 & -1 \end{array} \right] \tag{14}$$

results after elimination of the boundary conditions in the linear system

$$A_h x_h = b_h \tag{15}$$

of size $n-1$. The grid vectors

$$\phi_h^\ell = \sin(\ell \pi x) \text{ for } 1 \leq \ell \leq n-1 \tag{16}$$

are eigenvectors of A_h corresponding to the eigenvalues

$$\lambda^\ell(A_h) = \frac{1}{h^2}(2 - 2\cos(\ell\pi h) - \kappa^2) = \frac{1}{h^2}(2 - 2\,\mathrm{c}_\ell - \kappa^2)\,, \tag{17}$$

where $\mathrm{c}_\ell = \cos(\ell\pi h)$. In what follows we will diagonalize the smoother $S_{h,(\beta_1,\beta_2)}$ and two-grid operator $P_{h,H}$ defined by (10) and (12), respectively. This enables us to derive closed form expressions for the eigenvalues of the two-grid preconditioner $B_{h,H,(\beta_1,\beta_2)}$ defined by (13) in a subsequent stage. We therefore proceed in the standard way [31] and reorder the eigenvectors according to

$$V_h = [\phi_h^1, \phi_h^{n-1}, \phi_h^2, \phi_h^{n-2}, ..., \phi_h^{n/2-1}, \phi_h^{n/2}]. \tag{18}$$

This basis brings A_h into a block diagonal form that can be written as

$$A_h = \left[A_h^\ell\right]_{1\le\ell\le n/2}\,, \tag{19}$$

where for $1 \le \ell \le n/2-1$, A_h^ℓ is the 2×2 diagonal block

$$A_h^\ell = \begin{bmatrix} \frac{1}{h^2}(2-2\,\mathrm{c}_\ell-\kappa^2) & 0 \\ 0 & \frac{1}{h^2}(2+2\,\mathrm{c}_\ell-\kappa^2) \end{bmatrix}, \tag{20}$$

and $A_h^{n/2}$ is the 1×1 block

$$A_h^{n/2} = \frac{2}{h^2} - k^2\,. \tag{21}$$

4.1 Smoothing Analysis

The vectors (18) are eigenvectors of the preconditioner $M_{h,(\beta_1,\beta_2)}$ corresponding to the eigenvalues

$$\lambda_h^\ell(M_{h,(\beta_1,\beta_2)}) = \frac{1}{h^2}[2-2\,\mathrm{c}_\ell-(\beta_1-\iota\beta_2)\kappa^2]\,. \tag{22}$$

The eigenvalues of the smoother $S_{h,(\beta_1,\beta_2)}$ are therefore given by

$$\lambda_h^\ell(S_{h,(\beta_1,\beta_2)}) = 1 - \frac{2-2\,\mathrm{c}_\ell-\kappa^2}{2-2\,\mathrm{c}_\ell-(\beta_1-\iota\beta_2)\kappa^2}. \tag{23}$$

These eigenvalues for $(\beta_1,\beta_2) = (1, 0.5)$ are plotted in Figures 2(a), 2(b) and 2(c) for $k = 30$, $k = 60$ and $k = 120$, respectively. In these plots the meshwidth h is chosen in such a way to satisfy the condition (8). This figure clearly illustrates that the spectral radius is bounded by 1 and that the spectrum has more eigenvalues around the origin as the wavenumber increases.

The diagonalization of $S_{h,(\beta_1,\beta_2)}$ in the basis (18) results in the 2×2 blocks

$$S_{h,(\beta_1,\beta_2)}^\ell = \begin{bmatrix} 1-\frac{2-2\,\mathrm{c}_\ell-\kappa^2}{2-2\,\mathrm{c}_\ell-(\beta_1-\iota\beta_2)\kappa^2} & 0 \\ 0 & 1-\frac{2+2\,\mathrm{c}_\ell-\kappa^2}{2+2\,\mathrm{c}_\ell-(\beta_1-\iota\beta_2)\kappa^2} \end{bmatrix}, \tag{24}$$

for $1 \le \ell \le n/2-1$ and the 1×1 block

$$S_{h,(\beta_1,\beta_2)}^{n/2} = 1 - \frac{2-\kappa^2}{2-(\beta_1-\iota\beta_2)\kappa^2}\,. \tag{25}$$

4.2 Coarse Grid Correction Analysis

As restriction operator I_h^H we will use the full weighting operator with stencil

$$[I_h^H] = \left[\begin{array}{ccc} \frac{1}{4} & \frac{1}{2} & \frac{1}{4} \end{array}\right], \tag{26}$$

and as prolongation operator I_H^h linear interpolation. Given the fact that the basis (18) diagonalizes the linear interpolation operator $I_H^h \in \mathbb{R}^{n\times(\frac{n}{2}-1)}$ into blocks

$$(I_H^h)^\ell = \left[\begin{array}{cc} \frac{1}{2}(1+\mathrm{c}_\ell) & -\frac{1}{2}(1-\mathrm{c}_\ell) \end{array}\right], \tag{27}$$

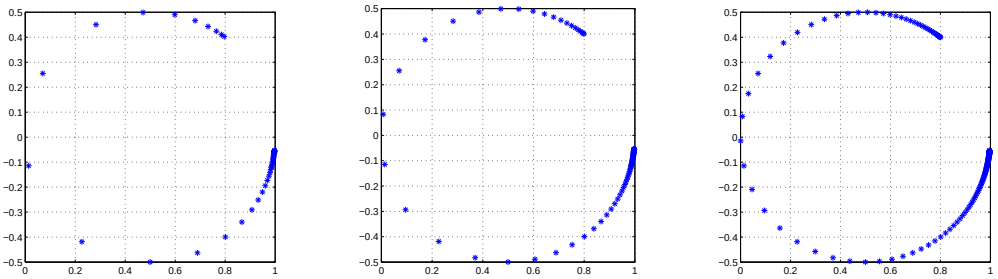

(a) $\sigma(S_{h,(1,0.5)})$ for $k = 30$ (b) $\sigma(S_{h,(1,0.5)})$ for $k = 60$ (c) $\sigma(S_{h,(1,0.5)})$ for $k = 120$

Figure 2: Spectrum of the SLP smoother $S_{h,(1,0.5)}$ given by (23) for different values of the wavenumber k.

for $1 \leq \ell \leq n/2 - 1$ and $(I_H^h)^{n/2} = 0$, and that the intergrid transfer operators are related by $I_H^h = (I_h^H)^T$, the 1×1 diagonal blocks of the Galerkin coarse grid operator A_H can shown to be equal to

$$A_H^\ell = (I_h^H)^\ell A_h^\ell (I_H^h)^\ell = \frac{2(1 - c_\ell^2) - \kappa^2(1 + c_\ell^2)}{2h^2}, \tag{28}$$

for $1 \leq \ell \leq n/2 - 1$ and $(A_H)^{n/2} = 0$. For the eigenvalues of the coarse grid correction operator $P_{h,H}$ this implies that

$$\begin{aligned} P_{h,H}^\ell &= I - (I_H^h)^\ell (A_H^\ell)^{-1} (I_h^H)^\ell A_h^\ell \\ &= \begin{bmatrix} 1 - \frac{\frac{1}{2}(1 + \mathrm{c}_\ell)^2(-2 + 2\,\mathrm{c}_\ell + \kappa^2)}{2(\mathrm{c}_\ell^2 - 1) + \kappa^2(\mathrm{c}_\ell^2 + 1)} & \frac{\frac{1}{2}(\mathrm{c}_\ell^2 - 1)(2 + 2\,\mathrm{c}_\ell - \kappa^2)}{2(\mathrm{c}_\ell^2 - 1) + \kappa^2(\mathrm{c}_\ell^2 + 1)} \\ \frac{\frac{1}{2}(\mathrm{c}_\ell^2 - 1)(-2 + 2\,\mathrm{c}_\ell + \kappa^2)}{2(\mathrm{c}_\ell^2 - 1) + \kappa^2(\mathrm{c}_\ell^2 + 1)} & 1 + \frac{\frac{1}{2}(\mathrm{c}_\ell^2 - 1)(2 + 2\,\mathrm{c}_\ell - \kappa^2)}{2(\mathrm{c}_\ell^2 - 1) + \kappa^2(1 + \mathrm{c}_\ell^2)} \end{bmatrix}, \end{aligned} \tag{29}$$

for $1 \leq \ell \leq n/2 - 1$ and $P_{h,H}^{n/2} = 0$. This real valued operator is a projection, and has 0 and 1 as eigenvalues.

4.3 Two-Grid Analysis

Combining results of the two previous subsections, we conclude that the operator $B_{h,H,(\beta_1,\beta_2)}$ has 0 as eigenvalue of multiplicity $n/2$ and $n/2 - 1$ eigenvalues of the form

$$\lambda^\ell(B_{h,H,(\beta_1,\beta_2)}) = \frac{a_\ell + \iota b_\ell}{c_\ell + \iota d_\ell} \qquad 1 \leq \ell \leq n/2 - 1, \tag{30}$$

where

$$
\begin{aligned}
a_\ell &= (\beta_2^2\,\mathrm{c}_\ell^2 + \beta_2^2 - \beta_1^2 + \mathrm{c}_\ell^2\beta_1 + \beta_1 - \beta_1^2\,\mathrm{c}_\ell^2)\kappa^6 + (2\,\mathrm{c}_\ell^2 - 2 + 2\beta_1^2 - 2\,\mathrm{c}_\ell^2\beta_1^2 + 2\beta_2^2\,\mathrm{c}_\ell^2)\kappa^4 \\
&\quad +(4 - 4\beta_1 - 8\,\mathrm{c}_\ell^2 + 4\,\mathrm{c}_\ell^4 + 8\beta_1\,\mathrm{c}_\ell^2 - 4\beta_1\,\mathrm{c}_\ell^4)\kappa^2 \\
b_\ell &= (2\beta_1\beta_2 - \beta_2 - \mathrm{c}_\ell^2\beta_2 + 2\beta_1\,\mathrm{c}_\ell^2\beta_2 - \beta_1^2\,\mathrm{c}_\ell^2)\kappa^6 + (4\beta_1\,\mathrm{c}_\ell^2\beta_2 - 4\beta_1\beta_2)\kappa^4 \\
&\quad +(4\beta_2 - 8\,\mathrm{c}_\ell^2\beta_2 + 4\beta_2\,\mathrm{c}_\ell^4)\kappa^2 \\
c_\ell &= (\beta_2^2 - \beta_1^2 + \beta_2^2\,\mathrm{c}_\ell^2 - \beta_1^2\,\mathrm{c}_\ell^2)\kappa^6 + (4\,\mathrm{c}_\ell^2\beta_1 + 2\beta_1^2 - 2\beta_2^2 + 4\beta_1 - 2\beta_1^2\,\mathrm{c}_\ell^2 + 2\beta_2^2\,\mathrm{c}_\ell^2)\kappa^4 \\
&\quad +(8\,\mathrm{c}_\ell^2\beta_1 - 4 - 8\beta_1 + 4\,\mathrm{c}_\ell^4)\kappa^2 + (8\,\mathrm{c}_\ell^4 - 16\,\mathrm{c}_\ell^2 + 8) \\
d_\ell &= (2\beta_1\beta_2 + 2\beta_1\beta_2\,\mathrm{c}_\ell^2)\kappa^6 + (4\beta_1\,\mathrm{c}_\ell^2\beta_2 - 4\beta_1\beta_2 - 4\beta_2 - 4\,\mathrm{c}_\ell^2\beta_2)\kappa^4 + (8\beta_2 - 8\,\mathrm{c}_\ell^2\beta_2)\kappa^2.
\end{aligned}
$$

These eigenvalues for $(\beta_1, \beta_2) = (1, 0.5)$ are plotted in Figures 3(a), 3(b) and 3(c) for $k = 30$, $k = 60$ and $k = 120$, respectively. As in Figure 2, the meshwidth h was chosen in accordance to (8). This figure shows that the spectrum is clustered around $(1, -0.1)$ surrounded by a few outliers. Increasing the wave number no longer causes the eigenvalues to accumulate at the origin. Instead, it makes the outliers go further away from the cluster. This spectrum is favorable for convergence of GMRES, as outliers are well approximated by the Ritz values in the first few iterations. This is illustrated in Figures 4(a), 4(b) and 4(c) where the Ritz values after 4 GMRES iterations are plotted.

Expression (30) additionally offers insight on how values for (β_1, β_2) affect the performance of the two-grid preconditioner. In particular, it allows to asses the effect of making the preconditioner $M_{h,(\beta_1,\beta_2)}$ more diagonally dominant by increasing β_2. In Figures 5(a), 5(b), 5(c), the spectrum $\sigma(B_{h,H,(\beta_1,\beta_2)})$ for $\kappa = 0.625$ and $\beta_1 = 1$ is plotted for $\beta_2 = .5$, $\beta_2 = .75$ and $\beta_2 = 1$, respectively. These figures show that the spectrum remains virtually unchanged as β_2 increases. This opens promising perspectives on obtaining a good preconditioner at very low cost.

Expression (30) finally allows to study how changing the number of grid points per wave length $1/\kappa$ affects the spectrum of the two-grid precondtioner. In Figures 6(a), 6(b) and 6(c) we plotted the spectrum $\sigma(B_{h,H,(1,0.5)}$ for $\kappa = 0.625$, $\kappa = 0.312$ and $\kappa = 0.156$, respectively. These figures show that the spectrum becomes more clustered and therefore the linear system is easier to solve by Krylov subspace solvers as the number of grid points per wavelength increases.

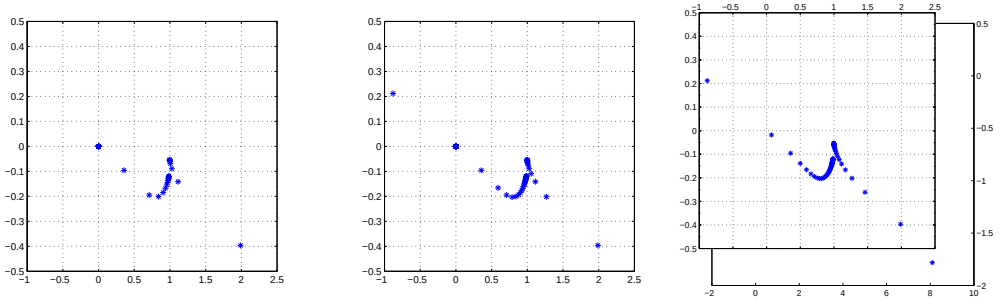

(a) $\sigma(B_{h,H,(1,0.5)})$ for $k = 30$ (b) $\sigma(B_{h,H,(1,0.5)})$ for $k = 60$ (c) $\sigma(B_{h,H,(1,0.5)})$ for $k = 120$

Figure 3: Spectrum of the two-grid preconditioner $B_{h,H,(1,0.5)}$ given by (30) for different values of the wavenumber k.

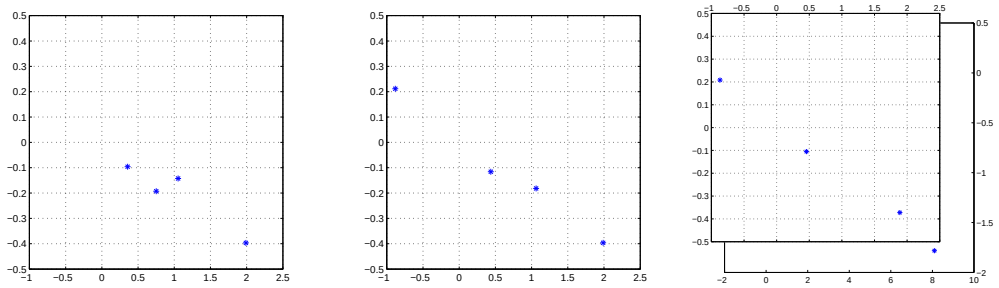

(a) Ritz Values for $k = 30$ (b) Ritz values for k=60 (c) Ritz values for k=120

Figure 4: Ritz values after 4 iterations GMRES preconditioned by $B_{h,H,(1,0.5)}$ for different values of the wavenumber k.

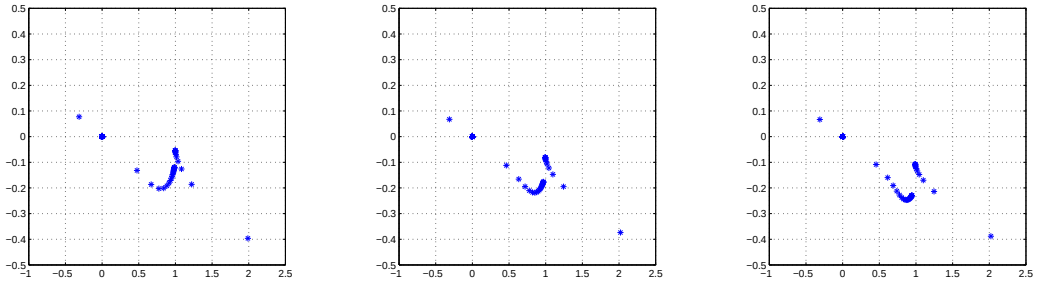

(a) $\beta_2 = .5$ (b) $\beta_2 = .75$ (c) $\beta_2 = 1$

Figure 5: Spectrum of the two-grid preconditioner $B_{h,H,(\beta_1,\beta_2)}$ given by (30) for $\kappa = 0.625$, $\beta_1 = 1$ and for different values of the imaginary shift β_2.

5 Numerical Experiments

In this section we perform numerical experiments on the constant and non-constant wave number problems described in Section 2 aiming at two goals. First we show in Subsection 5.1 that using deflation allows to make the SLP precondioner more diagonally dominant by increasing the imaginary part in the shift (β_2) without paying any penalty in the number of GMRES iterations. Subsequently we show in Subsection 5.2 and Subsection 5.3 that using deflation results in a number of GMRES iterations that remains constant as the wavenumber increases. In these latter experiments we use $(\beta_1, \beta_2) = (1, 0.5)$. In Subsection 5.2 we also show that the use of Dirichlet boundary conditions in the Fourier analysis is justified. Both the SLP preconditioner and coarse-grid linear system appearing in the deflation operator are inverted exactly. The full GMRES iterations are terminated if the scaled residual satisfied the relation

$$\frac{\|b_h - A_h x\|_2}{\|b_h\|_2} \leq 10^{-7}\,. \tag{31}$$

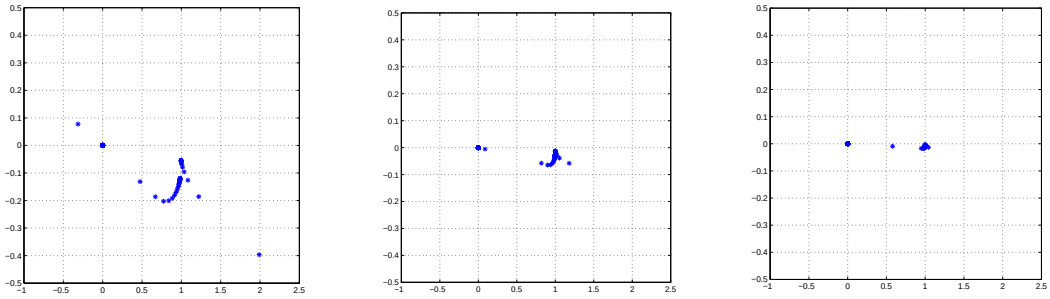

(a) $\kappa = 0.625$ (b) $\kappa = 0.312$ (c) $\kappa = 0.156$

Figure 6: Spectrum of the two-grid preconditioner $B_{h,H,(1,0.5)}$ given by (30) for different values of κ, .

5.1 Influence of the Imaginary Part of the Shift

In Figures 7(a) and 7(b) we plotted the required number of GMRES iterations to solve the constant and non-constant wavenumber problem with first order Sommerfeld boundary conditions for $k = 50$ and $f = 30$ as a function of the imaginary shift β_2, respectively. The meshwidth h was again chosen such that the requirement requirement (8) is fulfilled. We have chosen $\beta_1 = 1$ and allowed β_2 to vary between 0 and 1. For $\beta_2 = 0$, the SLP preconditioner coincides with the discrete Helmholtz operator, and the algorithm converges in a single iteration. The figures show that without deflation, the number of GMRES iterations increases with β_2. As observed in e.g. [27], this is due to the fact that the SLP preconditioner differs more from the discrete operator as β_2 increases. More interestingly, the figures shows that with deflation, the required number of GMRES iterations remains constant in β_2. These graphs confirm the Fourier analysis results in the previous section and the perspective of obtaining a good preconditioner at very low cost.

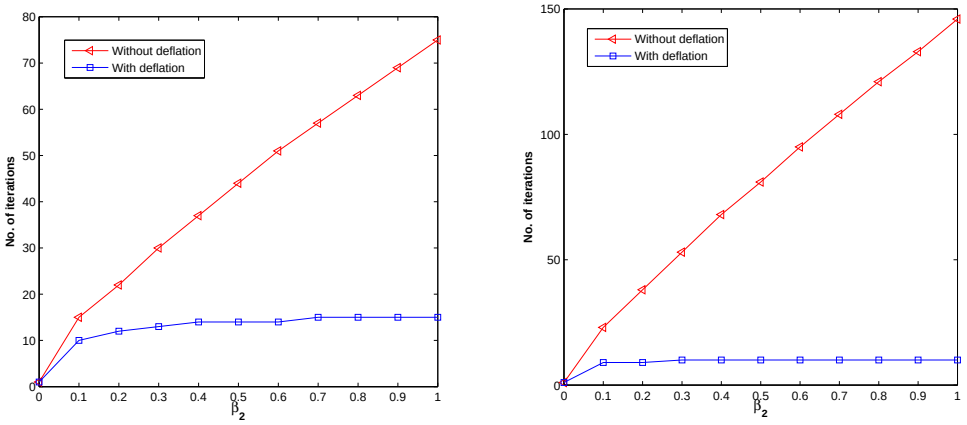

(a) Constant wavenumber problem (b) Non-constant wavenumber problem

Figure 7: Number of GMRES iterations for the constant and non-constant wavenumber problem for $k = 50$ and $f = 30$ versus the imaginary part of the shift β_2.

5.2 Constant Wavenumber Problem

In Figure 8 we plotted the spectrum of the SLP $S_{h,(1,.5)}$ and two-grid preconditioner $B_{h,H,(1,.5)}$ for the constant wavenumber problem with Sommerfeld boundary conditions for $k = 50$ and $n = 80$. In these figures we used circles to highlight the distance from the cluster of eigenvalues from the origin. Comparing Figure 8(a) with its equivalent for the Dirichlet boundary conditions in Figure 2 confirms earlier findings in i.e. [27] that the problem with Sommerfeld boundary conditions is easier to solve. This is due to the damping that the boundary conditions introduce. This justifies the use of Dirichlet boundary to analyze the worst-case scenario by a Fourier analysis. Figure 8(b) shows that the use of deflation results in a spectrum much more favorable for the convergence of GMRES. Indeed, the cluster of eigenvalues of $B_{h,H,(1,.5)}$ lies further away from the origin than the spectrum of $S_{h,(1,.5)}$. How the spectra shown in Figure 8 translate into number of iterations for different wavenumbers is shown in Table 1 and Table 2.

In Table 1 and Table 2 we give the number of GMRES iterations required to solve the constant wavenumber problem with Dirichlet and Sommerfeld boundary conditions for a range of wavenumbers and number of elements, respectively. We contrast the variants with and without deflation. In both tables only the number of elements on and below the diagonal highlighted in bold suffice to meet the requirement of 20 mesh points per wave length, which is more stringent than the condition (8). For both Dirichlet and Sommerfeld boundary conditions, the number of iterations for fixed k decreases with increasing n. This confirms our Fourier analysis. Comparing both tables confirms the claim that the problem with Dirichlet boundary conditions acts as a worst case for the problem with Sommerfeld boundary conditions. The tables also show that while without the use of deflation the number of GMRES iterations depends on the wavenumber, this is clearly no longer the case if deflation is used. These tables therefore proofs the fact that our solver is scalable.

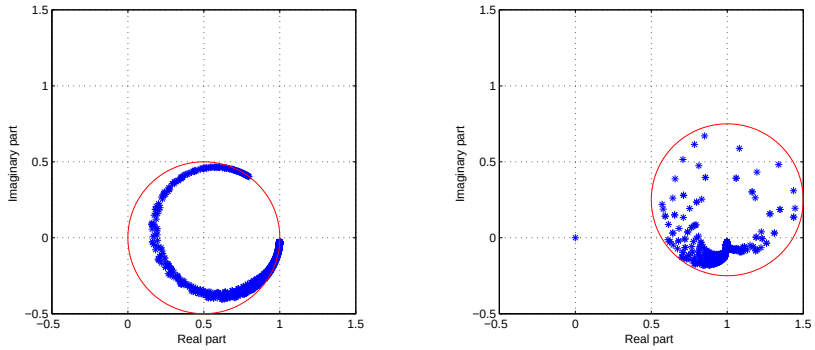

(a) $\sigma(S_{h,(1,.5)})$ (b) $\sigma(B_{h,H,(1,.5)})$

Figure 8: Spectrum of the SLP $S_{h,(1,.5)}$ and two-grid preconditioner $B_{h,H,(1,.5)}$ for the constant wavenumber problem with Sommerfeld boundary conditions for $k = 50$ and $n = 80$.

	$k=10$	$k=20$	$k=30$	$k=40$	$k=50$	$k=100$
$n=32$	**3/10**	8/17	17/31	35/50	52/80	13/14
$n=64$	3/10	**6/17**	10/30	17/47	24/63	221/252
$n=96$	3/10	5/17	**7/30**	11/46	15/62	209/220
$n=128$	3/10	5/17	6/30	**10/45**	11/62	90/196
$n=160$	3/10	4/17	5/30	8/45	**9/62**	65/194
$n=320$	2/10	3/17	4/30	5/45	6/61	**24/193**

Table 1: Number of GMRES iterations for the constant wavenumber problem with Dirichlet boundary conditions for different wave numbers and grid resolutions using the preconditioner $S_{h,(1,0.5)}$ with / without deflation.

	$k=10$	$k=20$	$k=30$	$k=40$	$k=50$	$k=100$
$n=32$	**5/10**	8/17	14/28	26/44	42/70	13/14
$n=64$	4/10	**6/17**	8/28	12/36	18/45	173/163
$n=96$	3/10	5/17	**7/27**	9/35	12/43	36/97
$n=128$	3/10	4/17	6/27	**7/35**	9/43	36/85
$n=160$	3/10	4/17	5/27	6/35	**8/43**	25/82
$n=320$	3/10	4/17	4/27	5/35	5/42	**10/80**

Table 2: Number of GMRES iterations for the constant wavenumber problem with Sommerfeld boundary conditions for different wave numbers and grid resolutions using the preconditioner $S_{h,(1,0.5)}$ with / without deflation.

5.3 Non-Constant Wavenumber Problem

In this subsection we consider the non-constant wavenumber problem. As in the previous subsection, we give in Table 3 the required number of GMRES iterations for different frequencies and mesh sizes with and without deflation. This table shows that even in the case of contrast in the wave number the solver remains scalable.

	$freq=10$	$freq=20$	$freq=30$	$freq=40$	$freq=50$
74×124	**7/33**	20/60	79/95	267/156	490/292
148×248	5/33	**9/57**	17/83	42/112	105/144
232×386	5/33	7/57	**10/81**	25/108	18/129
300×500	4/33	6/57	8/81	**12/105**	18/129
374×624	4/33	5/57	7/80	9/104	**13/128**

Table 3: Number of GMRES iterations for the non-constant wavenumber problem for different wave numbers and grid resolutions using the preconditioner $S_{h,(1,0.5)}$ with / without deflation.

6 Conclusions

In this paper we performed a Fourier analysis of a two-level variant of the multilevel Krylov method for the Helmholtz equation proposed by [1]. The distinct feature of the

solver analyzed is the two-grid deflation of the shifted Laplace preconditioner at each step of an outer Krylov subspace acceleration. Our analysis reveals two properties of the solver. The first is that with deflation the solver becomes scalable in the sense that the number of Krylov iterations iterations remains constant as the wave number increases. The second is that the shifted Laplace preconditioner can be made arbitrarily diagonally dominant by increasing the imaginary part of the shift without paying any penalty in the number of Krylov iterations. These properties are verified by numerical experiments on constant and non-constant wave number problems. Our algorithm therefore opens promising perspectives on solving the discrete Helmholtz on large scale.

References

[1] Y.A. Erlangga and R. Nabben. On a multilevel Krylov method for the Helmholtz equation preconditioned by shifted Laplacian. *Electronic Transaction on Num. Analysis (ETNA)*, 31:403–424, 2008.

[2] C.I. Goldstein A. Bayliss and E. Turkel. An iterative method for the Helmholtz equation. *Journal of Computational Physics*, 49:443 – 457, 1983.

[3] L.A. Laird and M.B. Giles. Preconditioned iterative solution of the 2d Helmholtz equation. Technical report, Comp. Lab. Oxford University UK, 2002. NA-02/12.

[4] Y.A. Erlangga, C. Vuik, and C.W. Oosterlee. On a class of preconditioners for solving the Helmholtz equation. *Appl. Numer. Math.*, 50(3-4):409–425, 2004.

[5] Y. A. Erlangga, C. W. Oosterlee, and C. Vuik. A novel multigrid based preconditioner for heterogeneous Helmholtz problems. *SIAM J. Sci. Comput*, 27:1471–1492, 2006.

[6] Y.A. Erlangga, C. Vuik, and C.W. Oosterlee. Comparison of multigrid and incomplete LU shifted-Laplace preconditioners for the inhomogeneous Helmholtz equation. *Applied Numerical Mathematics*, 56:648–666, 2006.

[7] B. Reps, W. Vanroose, and H. Bin Zubair. On the indefinite Helmholtz equation: Complex stretched absorbing boundary layers, iterative analysis, and preconditioning. *J. Comput. Phys.*, 229:8384–8405, November 2010.

[8] M. Bollhöfer, M. J. Grote, and O. Schenk. Algebraic multilevel preconditioner for the Helmholtz equation in heterogeneous media. *SIAM Journal on Scientific Computing*, 31:3781–3805, 2009.

[9] T. Airaksinen, E. Heikkola, A. Pennanen, and J. Toivanen. An algebraic multigrid based shifted-Laplacian preconditioner for the Helmholtz equation. *Journal of Computational Physics*, 226:1196 – 1210, 2007.

[10] Y. A. Erlangga and R. Nabben. Deflation and balancing preconditioners for Krylov subspace methods applied to nonsymmetric matrices. *SIAM J. Matrix Anal. Appl.*, 30:684–699, 2008.

[11] J. Zhu, X.W. Ping, R.S. Chen, Z.H. Fan, and D.Z. Ding. An incomplete factorization preconditioner based on shifted Laplace operators for FEM analysis of microwave structures. *Microwave and Optical Technology Letters*, 52:1036–1042, 2010.

[12] T. Airaksinen, A. Pennanen, and J. Toivanen. A damping preconditioner for time-harmonic wave equations in fluid and elastic material. *J. Comput. Phys.*, 228:1466–1479, March 2009.

[13] C.D. Riyanti, A. Kononov, Y.A. Erlangga, C. Vuik, C. Oosterlee, R.E. Plessix, and W.A. Mulder. A parallel multigrid-based preconditioner for the 3D heterogeneous high-frequency Helmholtz equation. *Journal of Computational Physics*, 224:431–448, 2007.

[14] R.E. Plessix. A Helmholtz iterative solver for 3D seismic-imaging problems. *Geophysics*, 72:SM185–SM194, 2007.

[15] R.E. Plessix. Three-dimensional frequency-domain full-waveform inversion with an iterative solver. *Geophysics*, 74(6):149–157, 2009.

[16] N. Umetani, S.P. MacLachlan, and C.W. Oosterlee. A multigrid-based shifted Laplacian preconditioner for a fourth-order Helmholtz discretization. *Numerical Linear Algebra with Applications*, 16:603–626, 2009.

[17] T. Airaksinen and S. Mönkölä. Comparison between the shifted-laplacian preconditioning and the controllability methods for computational acoustics. *J. Comput. Appl. Math.*, 234:1796–1802, July 2010.

[18] D. Osei-Kuffuor and Y. Saad. Preconditioning Helmholtz linear systems. *Appl. Numer. Math.*, 60:420–431, April 2010.

[19] M.B. van Gijzen, Y.A. Erlangga, and C. Vuik. Spectral analysis of the discrete Helmholtz operator preconditioned with a shifted Laplacian. *SIAM Journal on Scientific Computing*, 29:1942–1958, 2007.

[20] G. Samaey and W. Vanroose. An analysis of equivalent operator preconditioning for equation-free Newton-Krylov methods. *SIAM J. Numer. Anal.*, 48:633–658, 2010.

[21] K. Meerbergen and J.P. Coyette. Connection and comparison between frequency shift time integration and a spectral transformation preconditioner. *Numerical Linear Algebra with Applications*, 16:1–17, 2009.

[22] Y. A. Erlangga and R. Nabben. Algebraic multilevel Krylov methods. *SIAM Journal on Scientific Computing*, 31:3417–3437, 2009.

[23] Y.A. Erlangga. Advances in iterative methods and preconditioners for the Helmholtz equation. *Archives of Computational Methods in Engineering*, 15:37–66, 2008.

[24] R. E. Plessix and W. A. Mulder. Separation-of-variables as a preconditioner for an iterative Helmholtz solver. *Appl. Numer. Math.*, 44:385–400, 2003.

[25] Y. Saad and M.H Schultz. GMRES: a generalized minimal residual algorithm for solving nonsymmetric linear systems. *SIAM J. Sci. Stat. Comput.*, 7(3):856–869, 1986.

[26] H. A. van der Vorst. BI-CGSTAB: a fast and smoothly converging variant of bi-cg for the solution of nonsymmetric linear systems. *SIAM J. Sci. Stat. Comput.*, 13(2):631–644, 1992.

[27] Y.A. Erlangga. *A robust and effecient iterative method for numerical solution of Helmholtz equation.* PhD thesis, DIAM, TU Delft, 2005.

[28] M. M. M. Mardoche. Incomplete factorization-based preconditionings for solving the Helmholtz equation. *International Journal for Numerical Methods in Engineering*, 50:1077–1101, 2001.

[29] J.M. Tang, S.P. MacLachlan, R. Nabben, and C. Vuik. A comparison of two-level preconditioners based on multigrid and deflation. *SIAM. J. Matrix Anal. and Appl.*, 31:1715–1739, 2010.

[30] J. M. Tang. *Two Level Preconditioned conjugate gradient methods with applications to bubbly flow problems.* PhD thesis, DIAM, TU Delft, 2008.

[31] U. Trottenberg, C. W. Oosterlee, and A. Schüller. *Multigrid.* Academic Press, London, 2000.